Satellite Observations of AOD in 4 Northern Hemisphere Source Regions during the COVID-19 Pandemic

Sarah Elise Smith[1], Mingfang Ting[1], Yutian Wu[1], Cheng Zheng[1]

[1]Lamont-Doherty Earth Observatory, Columbia University, Palisades, NY, USA

Corresponding author: Sarah Elise Smith (sarahs@ldeo.columbia.edu)

Key Points:

- In Europe and the United States, record-low AOD persisted through the summer in 2020
- No significant pandemic-related decrease in AOD was observed in East & Central China
- In India, record-low AOD was primarily driven by natural sources

Abstract

Anticipated future reductions in aerosol emissions are expected to accelerate warming and substantially change precipitation characteristics. It is therefore vital to identify existing patterns and possible future pathways of anthropogenic aerosol reductions. The COVID-19 pandemic prompted abrupt, global declines in transportation and industrial activities, providing opportunities to study the aerosol effects of pandemic-driven emissions changes. Here, measures of aerosol optical depth (AOD) from two satellite instruments are used to characterize aerosol burdens in 2020 in four Northern Hemisphere source regions (East & Central China, the United States, India, and Europe). In most regions, spring and summer AOD was substantially lower than in previous years. However, in India and East & Central China, the COVID-19 AOD signature was eclipsed by sources of natural variability (dust) and a multi-year trend, respectively, suggesting that COVID-19-related emissions reductions account for substantially less of the 2020 anomalies in these regions than might otherwise be assumed.

Plain Language Summary

Aerosols are a suspension of small liquid or solid particles in the atmosphere that can influence air quality and climate. While some atmospheric aerosols have natural sources, many are generated by human activities and are expected to decline along with reductions in greenhouse gas emissions. The COVID-19 pandemic prompted abrupt cutbacks in transportation and industrial activities, which are major sources of human-generated aerosols. Here, we use data from two different types of satellite instruments to measure changes in aerosols in 2020 across four major aerosol-producing regions: East & Central China, India, Europe, and the United States. In most regions, measures of aerosols were much lower than in previous years; many months in the spring and summer showed record-low values. However, in some regions the reduction in aerosols related to COVID-19 was less than the reduction attributable to either multi-year efforts

to reduce emissions, or natural sources of aerosol variability. As the political, economic, and climatological implications of the COVID-19 pandemic continue to be examined, satellite observations provide essential context to on-the-ground reports of pandemic aerosol anomalies.

Index Terms & Keywords

305, 345, 1616, 1640, 3305

COVID-19, pandemic, lockdown, AOD

1 Introduction

Current estimates suggest that atmospheric aerosols contributed a global net radiative forcing of -.71 to -.14 Wm^{-2} to 2005-2015 surface temperatures (Bellouin et al., 2019). Efforts to reduce greenhouse gases (GHGs) are expected to result in fewer co-emitted aerosols, improving air quality but depleting the aerosol-offset to GHG-driven warming (Philipona et al., 2009; Szopa et al., 2021). As short-lived species, atmospheric aerosols are expected to decline more rapidly than long-lived GHGs, unmasking additional near-term warming even as emissions of long-lived forcers decline (Szopa et al., 2021). Aerosol radiative effects depend on spatially varying characteristics such as deposition rates, surface albedo, and aerosol composition. The precise impact of anticipated aerosol reductions therefore depends on complex and regionally inhomogeneous interactions between aerosols and hydrological cycles, atmospheric circulation, and geochemical cycles—interactions which can impact human livelihoods directly in addition to their effects on the radiative balance. While laboratory and modelling studies continue to constrain some of the uncertainties related to aerosol reductions, real-world observations provide crucial validation of model results, yet are rarely possible when considering anticipated future scenarios.

The COVID-19 pandemic prompted global reductions in transportation and industrial activities, providing an unprecedented opportunity to study the effects of aerosol reductions in multiple source regions. Bottom-up estimates of global CO_2 emissions range from 8.8 to ~25% reduction from 2019 values during the first half of 2020 (Forster et al., 2020; Le Quéré et al., 2020; Venter et al., 2020). Forster et al. (2020) also found 20% reductions in the sulfate aerosol precursor SO_2. In situ observations provide more localized information, as well as insights into potential feedbacks. Sharma et al. (2020) found substantial reductions in $PM_{2.5}$ in urban centers throughout India, while station data in several Chinese cities showed that an increase in secondary aerosol formation offset some emissions reductions early in the year (Chen et al., 2020; Huang et al., 2020). The Forster et al. (2020) methodology was used to develop emissions scenarios for the CovidMIP project, which has since been used to assess the climate impacts of COVID-19-related shutdowns (Lamboll et al., 2020; see also D'Souza et al., 2021; Fielder et al., 2021).

Bottom-up estimates of emissions reductions and their modelled effects need validation, yet most in situ observations during the pandemic are restricted

to surface-level observations in relatively populated localities. Satellite observations can be used to characterize aerosol burdens throughout the vertical column on a global scale with near-continuous coverage. Passive sensors such as MODIS are used to calculate column-integrated measures of aerosol optical depth (AOD) (Barnes et al., 2003), while LiDAR-based instruments such as CALIOP have the additional advantage of calculating extinction coefficients along a vertical profile (Winker et al., 2009). Processing the CALIOP retrievals also requires discrimination between seven different classifications of aerosol: dust, polluted dust, elevated smoke, polluted continental, clean continental, clean marine, and dusty marine, which can provide insight into relative contributions of natural and anthropogenic drivers of AOD variability.

Several studies have examined MODIS AOD values during the highly restrictive lockdown periods that characterized the early months of the pandemic, finding anomalously low AOD in India, Bangladesh, China, Europe, and the United States (Acharya et al. 2021; Bilal et al., 2021; Lal et al. 2020; Ranjan et al. 2020). Data from CALIOP have provided additional context to such lockdown observations; in Bangladesh and India, anomalously low dust contributed substantially to the low AOD signal in pre-monsoon months (Prijith & Srinivasulu 2021; Qiu et al., 2021). In sub-Saharan Africa, an increase in elevated smoke, possibly due to diminished enforcement of land management policies, characterized the early pandemic (Kganyago & Shikwambana, 2021; Qiu et al., 2021). To date, all satellite studies of the COVID-19 effect on AOD consider observations only during the first half of the year, despite economic disruptions persisting through the remainder of 2020 (e.g., Chowdhury et al., 2021; Onyeaka et al., 2021). Further, in many Northern hemisphere (NH) source regions climatological AOD values peak in mid- to late-summer, making observations of AOD during these months essential for quantifying the pandemic effect on aerosol burdens (e.g., Mehta et al., 2016). Finally, few studies contextualize pandemic AOD anomalies against the backdrop of longer-term trends, despite recent multi-year efforts to curtail air pollution in many source regions (e.g., Kuklinska et al., 2015; Ming et al. 2020; Zheng et al., 2020). Such background is important not only for appropriately quantifying the COVID-19 effect on AOD, but also for comparing the ancillary impacts of lifestyle changes to those of targeted public efforts to decrease air pollution.

More than half of the estimated reductions in black carbon and SO_2 in April of 2020 came from India, China, Europe, and the United States (Forester et al., 2020). As a result, in this study we consider the 2020 AOD signal in four NH regions: East & Central China, United States, India, and Europe. We consider not only observed anomalies relative to multi-year trends, but also the vertical profile of extinction coefficient anomalies as well as contributions from various aerosol subtypes.

2 Satellite Data and Methods

We obtained monthly mean AOD datasets generated from two satellite instruments, the NASA Moderate Resolution Imaging Spectroradiome-

ter MODIS (Aqua) and NASA Cloud-Aerosol LiDAR with Orthogonal Polarization CALIOP (Calipso). For both instruments we used level-3 gridded datasets: the global joint product (MYD08_M3, 1°x1°, AOD_550_Dark_Target_Deep_Blue) from MODIS and the tropospheric aerosol 'all sky' profile (CAL_LID_L3_Tropospheric_APro-Standard-V4-20/21, 2°x5°x60m) from CALIOP, which includes both AOD and extinction coefficient vertical profiles.

The CALIOP data product includes both day and night retrievals, which we treat as separate datasets. AOD and extinction coefficient contributions from three aerosol subtypes (dust, polluted dust, elevated smoke) are also available in the CALIOP datasets; we subtract these three subtypes from the all-aerosol data to create a composite subtype, 'continental,' which includes contributions from the two remaining aerosol subtypes available over land (clean continental, polluted continental), encompassing both carbonaceous aerosol from industrial sources as well as background/rural aerosol. Though MODIS and CALIOP products consider AOD at slightly different wavelengths (550 nm versus 532 nm, respectively), our analysis does not directly compare the datasets and wavelength disparity is expected to contribute relatively little to the significance of 2020 AOD anomalies. A considerable difference in viewing swath widths means that the sampling frequency of MODIS is substantially higher than CALIOP (1-2 days versus ~16 days).

Where AOD data was missing, we applied a 2D bilinear interpolation to fill the missing data, and excluded from the analysis any locations where more than 2 continuous pixels of data were missing at any point in the timeseries [Fig. S1]. In recent years the CALIOP LiDAR has produced low-energy laser shots over South America, leading to poor data quality in the region. Retrievals over this region have therefore been excluded from the CALIOP datasets used in this analysis. Noise in the CALIOP (day) vertical profiles can occur due to difficulties controlling for the effects of solar reflectance on LiDAR retrievals (Tackett et al., 2018). We therefore use the CALIOP (night) data to examine the contribution of aerosol subtypes to changes along the vertical profile.

3 Results & Discussion

3.2.1 Global reductions in 2020 AOD

Fig. 1 shows the 2020 annual mean AOD percent anomalies with respect to a 2007-2019 climatology from MODIS, CALIOP (night) and CALIOP (day). Despite differences in magnitude, all three datasets show anomalously low AOD in 2020 throughout much of the global land regions. While there are general reductions in AOD over much of the Eurasian landmass, the sign of the AOD anomalies within the Indian subcontinent remains inconsistent between datasets. A local enhancement of the negative AOD signature in Central China is evident in all three datasets, suggesting that a stronger local signal may be evident where COVID-19 first emerged. The maritime continent shows reductions in AOD as substantial as 40%, a similar magnitude to those observed in East Asia.

The Middle East and Iranian plateau also show 20 to 45% reductions in AOD, though the CALIOP data indicate that these anomalies are due to reductions in dust [Fig. S2].

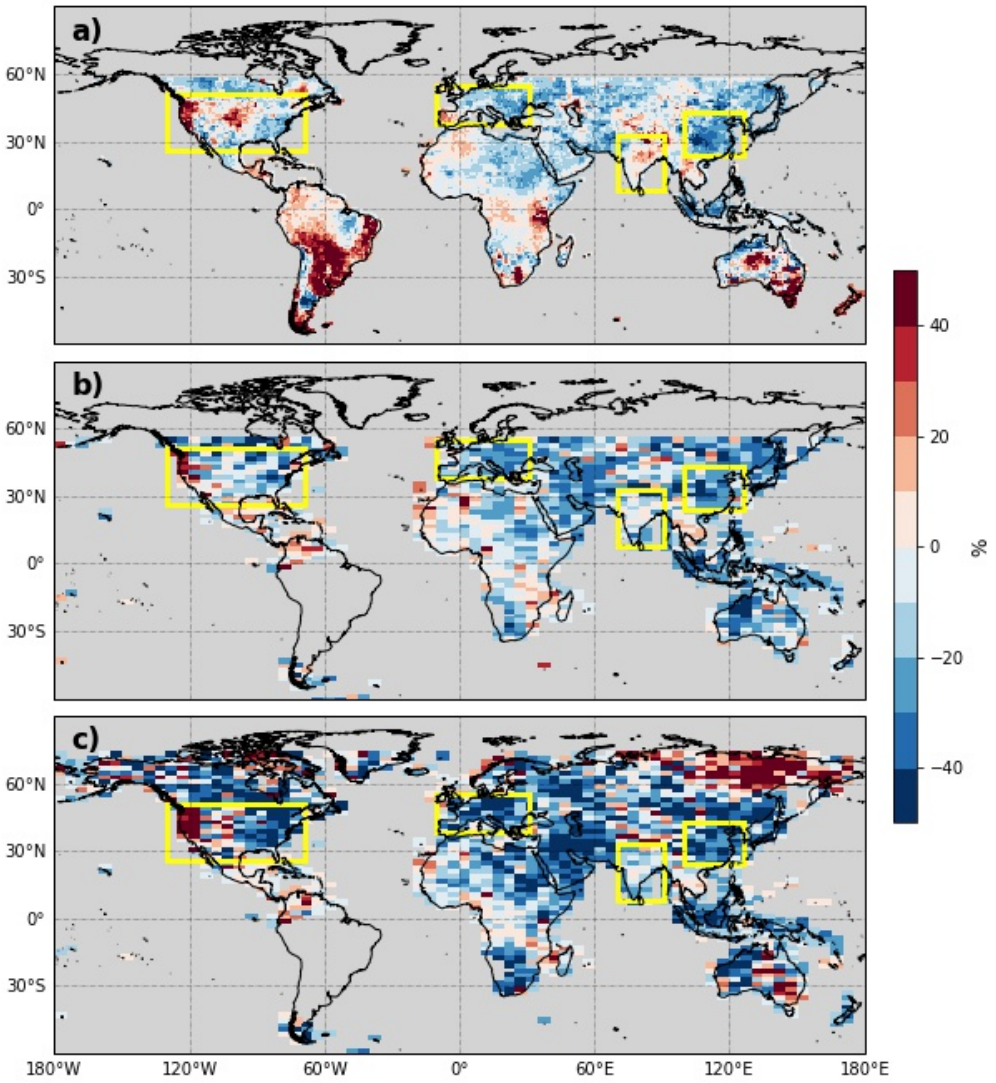

Fig. 1. 2020 annual percent anomalies relative to a 2007-2019 climatology for a) MODIS, b) CALIOP (night) and c) CALIOP (day). The regions examined below are delineated in yellow.

In Eastern North America and Western Europe, we observe 20 to 40% reductions in AOD. However, AOD increased in the western United States, consistent with record-breaking wildfires in this area during August and September. Spatial discrepancies of these positive anomalies between MODIS and CALIOP likely relate to the different sampling frequencies of the two instruments; transient and quick-moving, high-elevation smoke plumes are more likely to be observed in source regions by the more frequent sampling of MODIS.

Similarly, in Southern Africa the CALIOP data show 30 to 50% reductions in AOD while the MODIS dataset saw differences in sign throughout the region. Research supporting a COVID-19-related increase in biomass burning throughout sub-Saharan Africa could explain differences between the instruments (Kganyago & Shikwambana, 2021). While CALIOP data over South America are excluded from the analysis, MODIS data show increases in AOD from 40 to >50% in the Southern Amazon and Pampas. Other studies have found a lockdown-related increase in biomass burning in the Northern Amazon during the earliest months of the pandemic; our findings suggest that the possible contribution of biomass burning to Southern Amazonian AOD anomalies throughout 2020 is worthy of further investigation (Mendoza-Espinoza et al. 2020; Sanap 2021).

3.2 Changes in AOD Across Four Source Regions

To further determine how 2020 AOD changed across different source regions throughout the year, we select four main source regions for further analysis. These regions cover the land areas of Eastern & Central China (ECC, 24°-42°N 100°-125°E), the contiguous United States (US, 25°-50°N, 130°-70°W), India (IND, 8°-32°N, 70°-90°E), and Europe (EUR, 38°-54°N, 10°W-30°E), as indicated by the yellow boxes in Fig. 1. For each month in the sampling period (2007-2020), we calculate the area-weighted monthly AOD for the three datasets.

Fig. 2 shows that across all datasets and regions, 81% of months in 2020 showed below-average AOD, and 40% showed record-low AOD. For ECC, the US, and EUR, record-low values were mostly concentrated in the boreal spring and summer, when 72%, 67%, and 56% of months sampled showed record-lows, respectively. In both ECC and EUR, AOD values below the first quartile persisted for a majority of datasets from September to December, demonstrating that in these regions reductions endured well past the lockdown periods examined in previous studies. In contrast, the IND signal proved less persistent; 67% of months sampled in MAM showed record-lows, yet only 3 record-lows appear in the rest of the year. Still, the CALIOP datasets showed AOD below the first quartile through the remainder of the monsoon (JJAS) season, indicating that an enduring, if less extreme, signal continued through the late summer. In

the US, extreme wildfire events beginning in August overwhelmed the autumn AOD signal, producing record-high values in September and October. Though December saw a return to anomalously low AOD in the US, it is yet unclear whether this indicates the persistence of emissions-related reductions late into 2020.

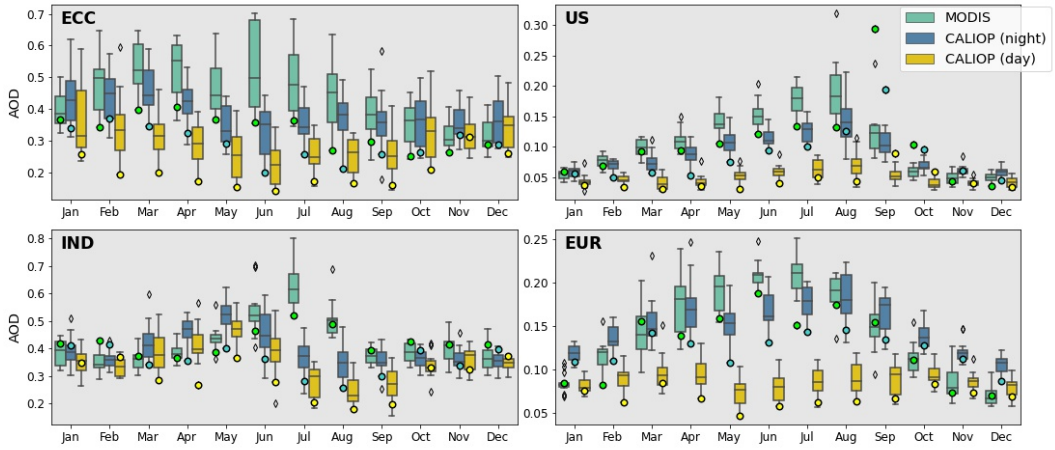

Fi

2. Distribution of 2007-2020 monthly mean AOD by dataset in East & Central China (ECC), the contiguous United States (US), India (IND) and Europe (EUR). Colored circles indicate 2020 values. Whiskers span up to 1.5x the interquartile range; outliers beyond this range are shown with diamond markers (2007-2019) or colored circles (2020).

For both the US and EUR, there is a clear seasonality of AOD that peaks in the summer months (May-August) but that is not reflected in the CALIOP (day) data for EUR, and is substantially dampened in the CALIOP (day) data for the US. Further analysis shows that the CALIOP (day) dataset poorly captures elevated smoke, which contributes ~20 and 35% to the mean AOD signature in the summer EUR and US CALIOP (night) datasets, respectively [Fig. S3]. Similarly, ECC AOD values characteristically peak in March and April in all datasets except CALIOP (day), which is occasioned by an underestimate of both elevated smoke and polluted dust by CALIOP (day) relative to CALIOP (night) [Fig. S3]. In IND, mean CALIOP AOD values peak at the end of the pre-monsoon season (May), while MODIS shows a maximum in July, reflecting a substantial change in instrument bias during the monsoon season (JJAS). Different handling of clouds by passive versus LiDAR instruments during the monsoon is a likely contributor to the differences between instruments (Kim et al., 2017).

Despite the anomalies in Fig. 1, none of the regions show substantial changes in

AOD seasonality in 2020; AOD minima and maxima for each region and dataset remain generally consistent with previous years, with the clear exception of the extreme September and October AOD values in the US. However, a dampening of the seasonality in all datasets in IND, as well as small deviations from the seasonal mean curve in spring in EUR and ECC, are apparent. While substantial, short-lived reductions to a dominant aerosol subtype could potentially alter AOD seasonality, the preservation of seasonality suggests that further analysis into the drivers of 2020 AOD anomalies is necessary.

3.3 Causes of Low 2020 AOD

While Fig. 2 suggests that AOD in all four source regions is at record-low values at some point in 2020, it is not clear whether these low values are driven by COVID-19-related anthropogenic aerosol reductions. Specifically, enhanced air quality regulations and thus a decreasing trend in AOD over this period could contribute to the low values, as could natural variability unrelated to the COVID shutdowns. To quantify monthly trends from a 13-year climatology, we calculate 3-month running means of observed regional AOD anomalies for each dataset, then determine the linear trend of these values for each month for the 2007 to 2019 period. Extrapolating from this linear trend, we then predict 3-month running mean AOD anomalies in 2020. Fig. 3 shows the observed (red) and predicted (blue) anomalies, as well as their differences, which correspond to the detrended AOD values.

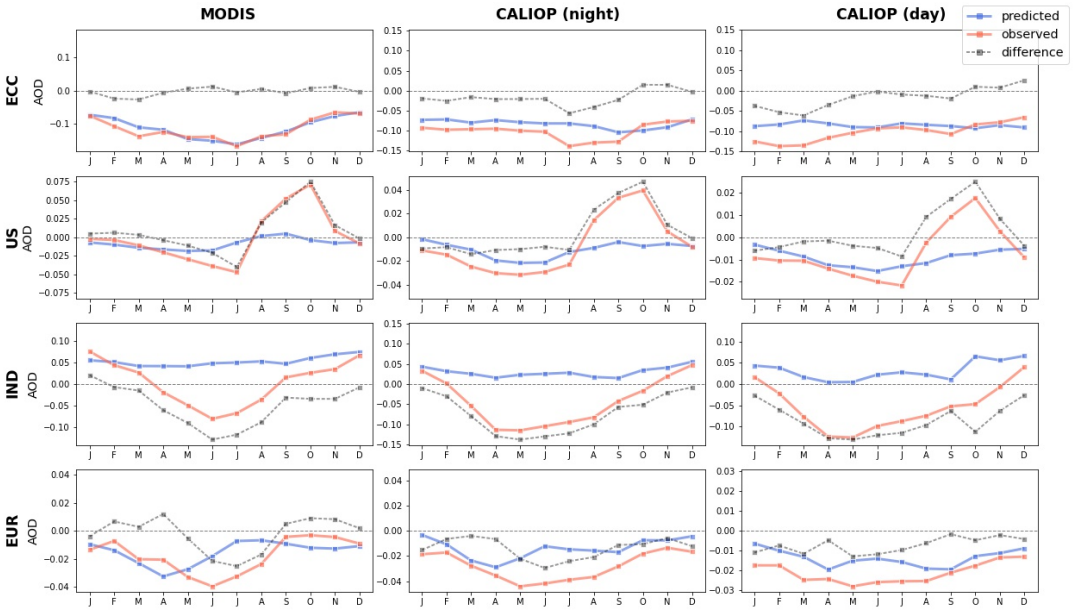

Fig. 3. Predicted (blue) and observed (red) 3-month running mean AOD anomalies in 2020, and their differences (i.e., detrended anomalies) for ECC, US, IND, and EUR.

Negative trends in AOD, indicated by the predicted AOD anomalies, characterize almost all months in ECC, US, and EUR (MODIS shows a negligibly positive trend in August and September in the US), while the IND trend is consistently positive. The positive IND trend is mostly steady throughout the year, contributing ~.05 AOD units to the detrended negative anomalies in much of 2020.

In ECC, the contribution of the trend to 2020 anomalies is up to an order of magnitude greater than EUR and the US, ranging from -.07 to -.15 AOD units. Despite slight differences between datasets, in ECC multi-year trends consistently eclipse the detrended anomalies. Other studies have noted that quantifying the AOD trend in ECC is challenging; a hastening of emissions reductions after 2014 suggests that a linear trend from 2007-2019 might not provide the most apt fit, yet with a relatively short time series the validity of higher order regressions is difficult to establish (e.g., Tao et al., 2020; van der A, 2017). However, investigation of the entire time series shows that monthly AOD anomalies in 2018 and 2019 were consistently and substantially negative, ranging from -.05 to -.14 AOD units, a similar magnitude to those observed in 2020 [Fig. S4]. Despite difficulties defining the ECC trend, we conclude that multi-year emissions reductions likely account for most, if not all, of the observed ECC anomalies in 2020.

In the US and EUR, negative trends are more modest, contributing from -.01 to -.02 AOD units in the US and up to -.03 in EUR to the 2020 AOD anomalies. The detrended anomalies appear mostly in late spring to summer, despite the most restrictive lockdowns occurring largely in March and April (Taylor, 2021). This observation contradicts earlier studies' assumptions that COVID-19-related AOD reductions would be most significant in the early spring, and may reflect seasonal differences in the trend as well as greater climatological values of anthropogenic AOD in the summer [Fig. S3] (e.g., Venter et al., 2020). Even where detrended anomalies were apparent, in many months the effect of the trends in the US and EUR was greater than the detrended anomalies, suggesting that for much of the year, longer term efforts to reduce emissions in these regions had a more substantial effect on 2020 AOD than COVID-related lifestyle changes.

To further determine the contributions of various aerosol types to the total 2020 AOD reductions, and to understand how the COVID-19 pandemic may have affected the vertical profile of aerosols, we compared the climatological mean annual vertical profiles (2007-2019) in each region to those of 2020, and decomposed the vertical profile anomalies to contributions from each aerosol subtype. Here we use the CALIOP (night) data to examine the contribution of aerosol subtypes to changes along the vertical profile (Fig. 4). Annual mean vertical profiles (Fig. 4) in ECC, the US, and EUR all show reductions in the lowest 2

km below the 95% confidence interval for the climatological mean, resulting in a flattening of the profiles. In the US and EUR, these negative anomalies are almost exclusively driven by reductions in continental aerosol. In ECC reductions are attributable to polluted dust and continental subtypes, indicating that in these regions 2020 reductions were primarily driven by anthropogenic sources. In contrast to the other three regions, changes in the IND annual mean vertical profile show a bimodal pattern, with slight reductions at the lowest levels (<.5 km) and another observable reduction from ~2-5 km. While all other regions show substantial negative anomalies in continental aerosol, IND in fact saw an increase consistent with the positive trend in continental aerosol noted in Fig. S5.

To determine when contributions from the different subtypes to 2020 extinction coefficient anomalies occurred, we calculated monthly extinction coefficient anomalies for each subtype and for the all-aerosol. In Fig. 4 we show monthly vertical profile anomalies from each subtype (columns labelled 'dust'-'continental') and the all-aerosol, which we normalized by the monthly mean climatological all-aerosol extinction coefficients. During the months of August through October (ASO), the effects from wildfires in the US are clearly evident in elevated smoke and polluted dust subtypes. In EUR, a similar signature in September and October appears above ~4 km, indicating transport of pyrogenic aerosols across the Atlantic. While in the US ASO all-aerosol is dominated by the effects of wildfire, reductions in continental aerosol in the lowest 2 km of the column persisted through these months, suggesting that reductions in anthropogenic aerosol continued throughout the remainder of 2020 but were masked by natural sources. In EUR, continental aerosol is consistently and substantially negative throughout 2020, showing that the persistence of AOD reductions in EUR is driven by enduring reductions in anthropogenic aerosol in the lowest levels of the troposphere.

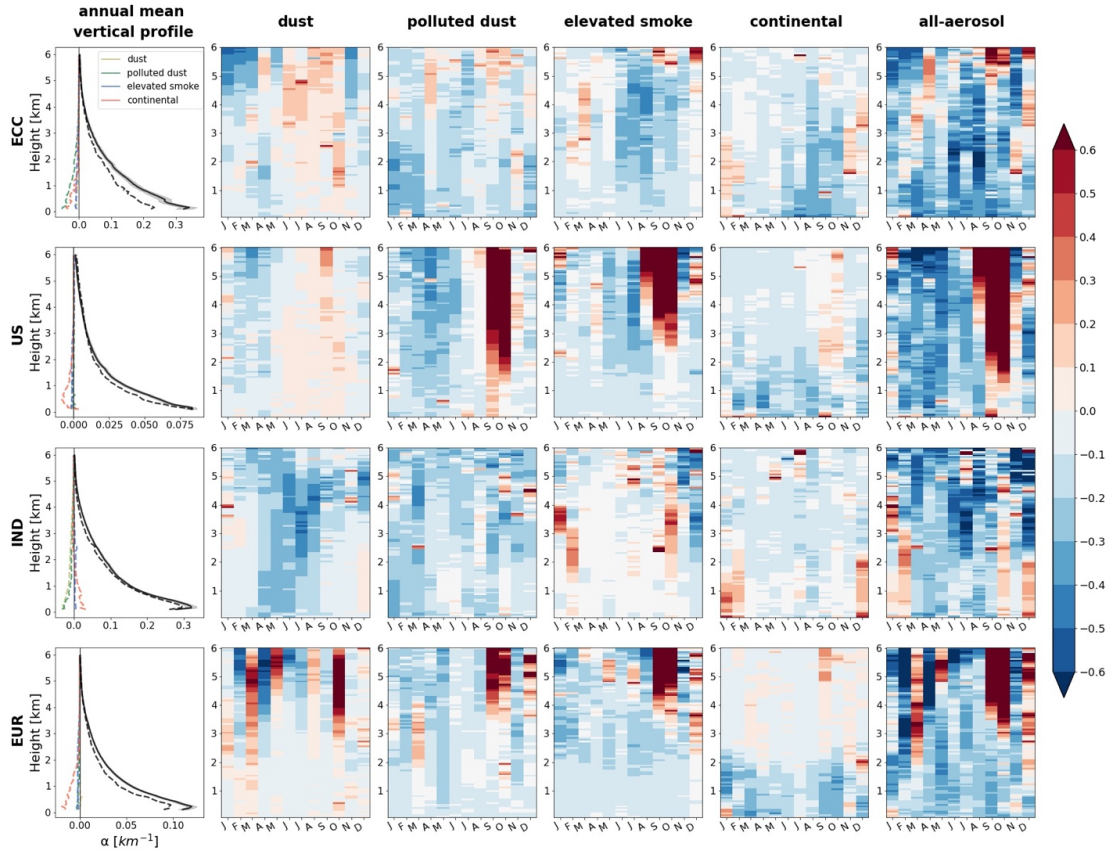

Fig. 4. Annual mean vertical profiles and normalized monthly extinction coefficient [ ] anomalies from CALIOP (night) for ECC, US, IND and EUR. Column titled 'Annual mean vertical profile' shows all-aerosol annual mean 2020 (black, dashed) and climatological (black, solid with shaded 95% confidence interval) vertical profiles, and the 2020 annual mean vertical profile anomalies of the four subtypes (colored, dashed). The colorbar for extinction coefficient anomalies for each subtype ('dust'-'continental') and 'all-aerosol' corresponds to the fraction of 2020 extinction coefficient anomalies relative to the all-aerosol climatological mean.

In ECC, changes in the annual mean vertical profile were driven by low anomalies in polluted dust and continental subtypes, with polluted dust dominating in January to March and continental dominating in June to September. As polluted dust is a mixture of dust and carbonaceous aerosol, continental aerosol subtype burdens can be modulated by dust availability. Anomalously low dust

in the early months of 2020 appears to have resulted in less mixing, which likely increased (decreased) the proportion of anthropogenic aerosols characterized as continental (polluted dust), independent of any other changes in emissions. However, the combined negative contribution from continental and polluted dust suggests that 2020 anomalies were primarily anthropogenic. However, as indicated earlier, a multi-year trend is likely the predominant cause of the anthropogenic signal in ECC.

Fig. 4 also shows that negative anomalies in IND were largely due to reductions in dust and polluted dust, with mid-year reductions in dust appearing most anomalous between 2-5 km. These were partially offset in the annual mean profile by positive anomalies in continental aerosols below 2 km, largely during the beginning and end of 2020. A positive trend in continental aerosol and the onset of negative detrended continental aerosol anomalies in mid-Spring may yet suggest a small COVID-19 signature in the region [Fig. S5]. Still, any such impact from COVID-19 was eclipsed by reductions in natural aerosol sources.

4 Conclusion

In the ECC, the US, IND, and EUR, anomalously low AOD persisted later into the year than early studies expected, and in fact the COVID-19 signal appears strongest in the post-lockdown periods. While trends in AOD are difficult to quantify, they nevertheless suggest that the COVID signature may be smaller than otherwise expected. In ECC, no COVID-19 AOD signature at the regional scale is apparent, as detrended anomalies are small relative to the trend. In IND, variability in natural aerosol sources (dust) dominated the observations. This may suggest a connection to the anomalously low dust over the Middle East, as prevailing winds would typically transport dust from the Arabian Peninsula and East Africa (Banerjee & Kumar, 2016; Ramaswamy et al., 2017). EUR and the US seem to show genuine COVID-19 signatures, even after natural aerosol sources and the effects of multi-year trends are taken into account. These COVID-19-related AOD anomalies are most observable in the lower part of the column (below 2 km), and the COVID-19 pandemic therefore resulted in a flattening of the aerosol vertical profile.

Our analysis suggests that satellite observations of AOD reductions during the 2020 COVID-19 pandemic may be more complex than initially thought. Even in regions with a notable COVID-19 signature, the effects from multi-year emissions trends often match or exceed those from COVID-19, suggesting that even extreme and universally adopted lifestyle changes may be no more effective in reducing emissions than policy-driven approaches. Whether economic differences, such as differing sectoral (e.g., transportation) contributions to a region's overall emissions, or the prevalence of livelihoods conducive to extended work-from-home arrangements, affected regional differences in 2020 AOD observations is worthy of consideration. However, it is clear from our analysis that anthropogenic aerosol emissions are decreasing in major source regions, particularly in China, even in the absence of a COVID-19 signature. Thus, their impacts on precipitation in these regions, as well as on accelerated greenhouse warming

through reduced aerosol cooling, are urgent issues that needs to be addressed.

Acknowledgements

Research for this manuscript was supported by the National Science Foundation Division of Atmospheric and Geospace Science and Office of Polar Programs, under awards AGS-1607348 and OPP-1825858.

Open Research (Availability Statement)

This study utilized the global joint product (MYD08_M3, 1°x1°, AOD_550_Dark_Target_Deep_Blue) from MODIS (Aqua) and the tropospheric 'all sky' profile (CAL_LID_L3_Tropospheric_APro-Standard-V4-20/21, 2°x5°x60m) from CALIOP satellite instruments.

The MODIS data can be accessed through the NASA LAADS DAAC archive: https://ladsweb.modaps.eosdis.nasa.gov/archive/allData/61/MYD08_M3/; we utilized all files contained within directories '2007/' to '2020/.' The variable 'AOD_550_Dark_Target_Deep_Blue_Combined_Mean_Mean' were used for AOD values and 'Deep_Blue_Aerosol_Optical_Depth_land_Mean_Mean' was used to mask ocean values for the MODIS data.

The CALIOP data can be accessed through the NASA OPeNDAP LARC archive: https://opendap.larc.nasa.gov/opendap/CALIPSO/LID_L3_Tropospheric_APro_AllSky-Standard-V4-20/contents.html; we utilized all files contained within the '2007/' to '2020/' directories. We used variables "AOD_Mean," AOD_Mean_Dust," "AOD_Mean_Polluted_Dust" and "AOD_Mean_Elevated_Smoke" for AOD values, and "Extinction_Coefficient_532_Mean," "Extinction_Coefficient_532_Mean_Dust," Extinction_Coefficient_532_Mean_Polluted_Dust," and "Extinction_Coefficient_532_Mean_Elevated_Sm for extinction coefficient profiles.

References

Acharya, P., Barik, G., Gayen, B. K., Bar, S., Maiti, A., Sarkar, A., et al. (2021). Revisiting the levels of Aerosol Optical Depth in south-southeast Asia, Europe and USA amid the COVID-19 pandemic using satellite observations. *Environmental Research*, *193*, 110514. https://doi.org/10.1016/j.envres.2020.110514

Banerjee, P., & Kumar, S. P. (2016). ENSO Modulation of Interannual Variability of Dust Aerosols over the Northwest Indian Ocean*. *Journal of Climate*, *29*(4), 1287–1303. https://doi.org/10.1175/JCLI-D-15-0039.1

Barnes, W. L., Xiong, X., Guenther, B. W., & Salomonson, V. (2003). *Development, characterization, and performance of the EOS MODIS sensors* (W. L. Barnes, Ed.; p. 337). https://doi.org/10.1117/12.504818

Bellouin, N., Quaas, J., Gryspeerdt, E., Kinne, S., Stier, P., Watson-Parris, D., et al. (2020). Bounding Global Aerosol Radiative Forcing of Climate Change. *Reviews of Geophysics*, *58*(1). https://doi.org/10.1029/2019RG000660

Bilal, M., Qiu, Z., Nichol, J. E., Mhawish, A., Ali, Md. A., Khedher, K. M., et al. (2021). Uncertainty in Aqua-MODIS Aerosol Retrieval Algorithms Dur-

ing COVID-19 Lockdown. *IEEE Geoscience and Remote Sensing Letters*, 1–5. https://doi.org/10.1109/LGRS.2021.3077189

Chen, Y., Zhang, S., Peng, C., Shi, G., Tian, M., Huang, et al. (2020). Impact of the COVID-19 pandemic and control measures on air quality and aerosol light absorption in Southwestern China. *Science of The Total Environment*, *749*, 141419. https://doi.org/10.1016/j.scitotenv.2020.141419

Chowdhury, P., Paul, S. K., Kaisar, S., & Moktadir, Md. A. (2021). COVID-19 pandemic related supply chain studies: A systematic review. *Transportation Research Part E: Logistics and Transportation Review*, *148*, 102271. https://doi.org/10.1016/j.tre.2021.102271

D'Souza, J., Prasanna, F., Valayannopoulos-Akrivou, L.-N., Sherman, P., Penn, E., Song, S., Archibald, A. T., & McElroy, M. B. (2021). Projected changes in seasonal and extreme summertime temperature and precipitation in India in response to COVID-19 recovery emissions scenarios. *Environmental Research Letters*, *16*(11), 114025. https://doi.org/10.1088/1748-9326/ac2f1b

Fiedler, S., Wyser, K., Rogelj, J., & van Noije, T. (2021). Radiative effects of reduced aerosol emissions during the COVID-19 pandemic and the future recovery. *Atmospheric Research*, *264*, 105866. https://doi.org/10.1016/j.atmosres.2021.105866

Forster, P. M., Forster, H. I., Evans, M. J., Gidden, M. J., Jones, C. D., Keller, et al. (2020). Current and future global climate impacts resulting from COVID-19. *Nature Climate Change*, *10*(10), 913–919. https://doi.org/10.1038/s41558-020-0883-0

Huang, L., Jiang, J. H., Tackett, J. L., Su, H., & Fu, R. (2013). Seasonal and diurnal variations of aerosol extinction profile and type distribution from CALIPSO 5-year observations: SEASONAL AND DIURNAL CHANGES OF AEROSOL. *Journal of Geophysical Research: Atmospheres*, *118*(10), 4572–4596. https://doi.org/10.1002/jgrd.50407

Kganyago, M., & Shikwambana, L. (2021). Did COVID-19 Lockdown Restrictions have an Impact on Biomass Burning Emissions in Sub-Saharan Africa? *Aerosol and Air Quality Research*, *21*(4), 200470. https://doi.org/10.4209/aaqr.2020.07.0470

Kim, M.-H., Omar, A. H., Vaughan, M. A., Winker, D. M., Trepte, C. R., Hu, Y., Liu, Z., & Kim, S.-W. (2017). Quantifying the low bias of CALIPSO's column aerosol optical depth due to undetected aerosol layers: Undetected Aerosols in CALIPSO AOD. *Journal of Geophysical Research: Atmospheres*, *122*(2), 1098–1113. https://doi.org/10.1002/2016JD025797

Kuklinska, K., Wolska, L., & Namiesnik, J. (2015). Air quality policy in the U.S. and the EU – a review. *Atmospheric Pollution Research*, *6*(1), 129–137. https://doi.org/10.5094/APR.2015.015

Lal, P., Kumar, A., Kumar, S., Kumari, S., Saikia, P., Dayanandan, A., Adhikari, D., & Khan, M. L. (2020). The dark cloud with a silver lining: Assessing the impact of the SARS COVID-19 pandemic on the global environment. *Science of The Total Environment*, *732*, 139297. https://doi.org/10.1016/j.scitotenv.2020.139297

Lamboll, R. D., Jones, C. D., Skeie, R. B., Fiedler, S., Samset, B. H., Gillett, N. P., Rogelj, J., & Forster, P. M. (2021). Modifying emissions scenario projections to account for the effects of COVID-19: Protocol for CovidMIP. *Geoscientific Model Development*, *14*(6), 3683–3695. https://doi.org/10.5194/gmd-14-3683-2021

Le Quéré, C., Jackson, R. B., Jones, M. W., Smith, A. J. P., Abernethy, S., Andrew, R. M., et al. (2020). Temporary reduction in daily global CO2 emissions during the COVID-19 forced confinement. *Nature Climate Change*, *10*(7), 647–653. https://doi.org/10.1038/s41558-020-0797-x

Mehta, M., Singh, R., Singh, A., Singh, N., & Anshumali. (2016). Recent global aerosol optical depth variations and trends—A comparative study using MODIS and MISR level 3 datasets. *Remote Sensing of Environment*, *181*, 137–150. https://doi.org/10.1016/j.rse.2016.04.004

Mendez-Espinosa, J. F., Rojas, N. Y., Vargas, J., Pachón, J. E., Belalcazar, L. C., & Ramírez, O. (2020). Air quality variations in Northern South America during the COVID-19 lockdown. *Science of The Total Environment*, *749*, 141621. https://doi.org/10.1016/j.scitotenv.2020.141621

Ming, Y., Loeb, N. G., Lin, P., Shen, Z., Naik, V., Singer, C. E., et al. (2021). Assessing the Influence of COVID-19 on the Shortwave Radiative Fluxes Over the East Asian Marginal Seas. *Geophysical Research Letters*, *48*(3). https://doi.org/10.1029/2020GL091699

Philipona, R., Behrens, K., & Ruckstuhl, C. (2009). How declining aerosols and rising greenhouse gases forced rapid warming in Europe since the 1980s: AEROSOL VERSUS GREENHOUSE GAS FORCING. *Geophysical Research Letters*, *36*(2), n/a-n/a. https://doi.org/10.1029/2008GL036350

Onyeaka, H., Anumudu, C. K., Al-Sharify, Z. T., Egele-Godswill, E., & Mbaegbu, P. (2021). COVID-19 pandemic: A review of the global lockdown and its far-reaching effects. *Science Progress*, *104*(2), 003685042110198. https://doi.org/10.1177/00368504211019854

Prijith, S. S., & Srinivasulu, J. (2021). Dominance of natural aerosols over India in pre-monsoon: Inferences from the lockdown effects. *CURRENT SCIENCE*, *120*(2), 8.

Qiu, Z., Ali, Md. A., Nichol, J. E., Bilal, M., Tiwari, P., Habtemicheal, B. A., et al. (2021). Spatiotemporal Investigations of Multi-Sensor Air Pollution Data over Bangladesh during COVID-19 Lockdown. *Remote Sensing*, *13*(5), 877. https://doi.org/10.3390/rs13050877

Ramaswamy, V., Muraleedharan, P. M., & Babu, C. P. (2017). Mid-troposphere transport of Middle-East dust over the Arabian Sea and its effect on rainwater composition and sensitive ecosystems over India. *Scientific Reports*, *7*(1), 13676. https://doi.org/10.1038/s41598-017-13652-1

Ranjan, A. K., Patra, A. K., & Gorai, A. K. (2020). Effect of lockdown due to SARS COVID-19 on aerosol optical depth (AOD) over urban and mining regions in India. *Science of The Total Environment*, *745*, 141024. https://doi.org/10.1016/j.scitotenv.2020.141024

Sanap, S. D. (2021). Global and regional variations in aerosol loading during COVID-19 imposed lockdown. *Atmospheric Environment*, *246*, 118132. https://doi.org/10.1016/j.atmosenv.2020.118132

Sharma, S., Zhang, M., Anshika, Gao, J., Zhang, H., & Kota, S. H. (2020). Effect of restricted emissions during COVID-19 on air quality in India. *Science of The Total Environment*, *728*, 138878. https://doi.org/10.1016/j.scitotenv.2020.138878

Szopa, S, Naik, V., Adhikary, B., Artaxo, P., Berntsen, T., Collins, W.D., et al., (2021) Short-Lived Climate Forcers Supplementary Material. In Climate Change 2021: The Physical Science Basis. Contribution of Working Group I to the Sixth Assessment Report of the Intergovernmental Panel on Climate Change [Masson-Delmotte, V., P. Zhai, A. Pirani, S.L. Connors, C. Péan, S. Berger, N. Caud, Y. Chen, L. Goldfarb, M.I. Gomis, M. Huang, K. Leitzell, E. Lonnoy, J.B.R. Matthews, T.K. Maycock, T. Waterfield, O. Yelekçi, R. Yu, and B. Zhou (eds.)]. Retrieved from https://www.ipcc.ch/

Tackett, J. L., Winker, D. M., Getzewich, B. J., Vaughan, M. A., Young, S. A., & Kar, J. (2018). CALIPSO lidar level 3 aerosol profile product: Version 3 algorithm design. *Atmospheric Measurement Techniques*, *11*(7), 4129–4152. https://doi.org/10.5194/amt-11-4129-2018

Tao, M., Wang, L., Chen, L., Wang, Z., & Tao, J. (2020). Reversal of Aerosol Properties in Eastern China with Rapid Decline of Anthropogenic Emissions. *Remote Sensing*, *12*(3), 523. https://doi.org/10.3390/rs12030523

Taylor, D. B. (2021, March 17). A Timeline of the Coronavirus Pandemic. *New York Times*. https://www.nytimes.com/article/coronavirus-timeline.html

van der A, R. J., Mijling, B., Ding, J., Koukouli, M. E., Liu, F., Li, Q., Mao, H., & Theys, N. (2017). Cleaning up the air: Effectiveness of air quality policy for SO_2; and NO_x; emissions in China. *Atmospheric Chemistry and Physics*, *17*(3), 1775–1789. https://doi.org/10.5194/acp-17-1775-2017

Venter, Z. S., Aunan, K., Chowdhury, S., & Lelieveld, J. (2020). COVID-19 lockdowns cause global air pollution declines. *Proceedings of the National Academy of Sciences*, *117*(32), 18984–18990. https://doi.org/10.1073/pnas.2006853117

Winker, D. M., Vaughan, M. A., Omar, A., Hu, Y., Powell, K. A., Liu, Z., Hunt, W. H., & Young, S. A. (2009). Overview of the CALIPSO Mission and CALIOP

Data Processing Algorithms. *Journal of Atmospheric and Oceanic Technology*, *26*(11), 2310–2323. https://doi.org/10.1175/2009JTECHA1281.1

Zheng, B., Geng, G., Ciais, P., Davis, S. J., Martin, R. V., Meng, J., et al. (2020). Satellite-based estimates of decline and rebound in China's CO_2 emissions during COVID-19 pandemic. *Science Advances*, *6*(49), eabd4998. https://doi.org/10.1126/sciadv.abd4998